ORIGINAL RESEARCH

Interleukin 10 Restores Gastric Emptying, Electrical Activity, and Interstitial Cells of Cajal Networks in Diabetic Mice

Kyoung Moo Choi,[1,*] Simon J. Gibbons,[1,*] Lei Sha,[1] Arthur Beyder,[1] Pieter-Jan Verhulst,[1] Gianluca Cipriani,[1] Jessica E. Phillips,[1] Anthony J. Bauer,[2] Tamas Ordog,[1] Jon J. Camp,[1] Xin Ge,[1] Adil E. Bharucha,[1] David R. Linden,[1] Joseph H. Szurszewski,[1] Purna C. Kashyap,[1] and Gianrico Farrugia[1]

[1]Enteric NeuroScience Program, Mayo Clinic School of Medicine, Rochester, Minnesota; [2]Department of Integrative Physiology and Pharmacology, Liberty University College of Osteopathic Medicine, Lynchburg, Virginia

SUMMARY

Interleukin 10 reversed delayed gastric emptying in diabetic mice. It increased heme oxygenase 1 expression and normalized electrical activity and networks of interstitial cells of Cajal in the stomach. Thus, interleukin 10 is a potential therapy for diabetic gastroparesis.

BACKGROUND & AIMS: Gastroparesis is a complication of diabetes characterized by delayed emptying of stomach contents and accompanied by early satiety, nausea, vomiting, and pain. No safe and reliable treatments are available. Interleukin 10 (IL10) activates the M2 cytoprotective phenotype of macrophages and induces expression of heme oxygenase 1 (HO1) protein. We investigated whether IL10 administration could improve gastric emptying and reverse the associated cellular and electrical abnormalities in diabetic mice.

METHODS: Nonobese diabetic mice with delayed gastric emptying were given either IL10 (0.1–1 μg, twice/day) or vehicle (controls). Stomach tissues were isolated, and sharp microelectrode recordings were made of the electrical activity in the gastric muscle layers. Changes to interstitial cells of Cajal (ICC), reduced nicotinamide adenine dinucleotide phosphate diaphorase, and levels and distribution of HO1 protein were determined by histochemical and imaging analyses of the same tissues.

RESULTS: Gastric emptying remained delayed in vehicle-treated diabetic mice but returned to normal in mice given IL10 (n = 10 mice; $P < .05$). In mice given IL10, normalization of gastric emptying was associated with a membrane potential difference between the proximal and distal stomach, and lower irregularity and higher frequency of slow-wave activity, particularly in the distal stomach. Levels of HO1 protein were higher in stomach tissues from mice given IL10, and ICC networks were more organized, better connected, and more evenly distributed compared with controls.

CONCLUSIONS: IL10 increases gastric emptying in diabetic mice and has therapeutic potential for patients with diabetic gastroparesis. This response is associated with up-regulation of HO1 and repair of connectivity of ICC networks. (Cell Mol Gastroenterol Hepatol 2016;2:454–467; http://dx.doi.org/10.1016/j.jcmgh.2016.04.006)

Gastroparesis is a complication of diabetes defined by delayed gastric emptying without obstruction that is accompanied by early satiety, nausea, vomiting, and pain.[1–3] No safe and reliable treatments are available.[4] Identification of the cellular changes associated with gastroparesis in human beings[5,6] and in mouse models of gastroparesis[7,8] have identified possible therapeutic targets. The nonobese diabetic (NOD) mouse in particular has proved to be a useful model of human diabetic gastroparesis.[7,9–11]

In previous studies using a noninvasive gastric emptying test, a proportion of diabetic NOD mice developed delayed emptying of solids while the remainder remained resistant to this complication.[11] Although most animals show loss of neuronal nitric oxide synthase upon the development of diabetes, the development of delayed gastric emptying was concurrent with reduced expression of the receptor tyrosine kinase, Kit, a marker for interstitial cells of Cajal (ICC).[7] This is consistent with studies showing impairment to ICC networks and loss of neuronal nitric oxide synthase in mice with long-standing diabetes.[9,10] Subsequent studies determined that animals resistant to the development of delayed emptying maintained high expression of heme oxygenase-1 (HO1) in alternatively activated M2-macrophages in stomach muscle layers.[7,8] In studies of the human gastric body, a correlation between the numbers of ICC and CD206-positive M2-macrophages was found.[12]

These studies have suggested that targeting HO1 may ameliorate diabetic gastroparesis. Indeed, treatment of

diabetic mice with delayed gastric emptying by inducing HO1 normalized gastric emptying and Kit expression levels.[7,8] These therapies were accompanied by increased numbers of HO1-positive, M2-macrophages in gastric muscularis propria.[8] Hemin (as Panhematin, Ovation Pharmaceuticals, Deerfield, IL) also up-regulates HO1 expression in human beings, although administration of hemin must be performed under close supervision.[13] These data suggest that HO1 is a promising therapeutic target for diabetic gastroparesis,[14] but treatment with hemin has significant disadvantages including the delivery method and side effects.

Consequently, a need exists to determine other modalities to target HO1. In the present study we tested interleukin 10 (IL10) as a treatment for delayed gastric emptying in NOD mice. The rationale was that IL10 expression is up-regulated during treatment by carbon monoxide (CO) of postoperative ileus in mice[15] and that IL10 had an obligatory role in postoperative intestinal recovery.[16] IL10 up-regulates HO1 expression[17] and is expressed at high levels in M2-macrophages. IL10 increases the numbers of M2-macrophages[18] directly and suppresses expression of M1-macrophages.[19] In addition, in diabetic mice with delayed emptying, IL10 messenger RNA levels were decreased.[8]

In previous studies on diabetic mice and rats, ICC networks and the electrical slow-wave activity that originates from ICC were absent or abnormal, especially in the distal antrum.[9,20] In human beings, electrical dysrhythmias also were reported in diabetic gastroparesis.[21–23] However, electrical properties and immunohistochemical differences were not comparatively studied in rodents with delayed gastric emptying or after normalization of gastric emptying. Thus, for the current study we made electrical recordings from multiple locations in the stomach of treated mice and subsequently immunolabeled for HO1 and Kit. Therefore, we were able to examine associations between gastric emptying of the mice and physiological and anatomic changes to the stomach, and the response of those changes to treatment with IL10.

## Materials and Methods
Animals and Experimental Design

Animal procedures were performed using protocols approved by the Mayo Clinic's Institutional Animal Care and Use Committee. Female NOD/ShiLtJ mice were used as previously described.[7,8,11] Blood glucose levels were measured every week until the onset of diabetes, after which point they were measured daily. Single drops of blood were collected from the vascular bundle located at the rear of the jaw bone of the mice. The amount of blood collected was monitored carefully to avoid anemia. Mice were considered diabetic when the glucose levels were higher than 250 mg/dL. The incidence of diabetes was 57% in this study. Subtherapeutic insulin (Lantus insulin glargine; Sanofi-Aventis US LLC, Bridgewater, NJ) was injected once daily intraperitoneally when the glucose levels were higher than 500 mg/dL to keep the diabetic mice alive, yet also keep the blood glucose levels between 400 and 600 mg/dL to allow complications of diabetes to develop. To determine

the levels of oxidative stress in the diabetic mice, the concentration of malondialdehyde (MDA) was measured in blood plasma. The concentration of thiobarbituric acid–reactive substances was calculated as malondialdehyde equivalents using a commercial kit (Oxi-Tek; Zeptometrix Corp, Buffalo, NY). Five microliters of plasma sample was mixed with an equal volume of sodium dodecyl sulfate solution and 125 μL of 5% thiobarbituric acid/acetic acid reagent. Samples were incubated for 60 minutes at 95°C. After centrifugation at 1600g, the absorbances of supernatants from samples were read at 532 nm using a spectrophotometer (NanoDrop Technology, Wilmington, DE).

Gastric emptying of solids was measured using a ^{13}[C]-octanoic acid breath test.[11] Three baseline values of times to half maximal emptying ($T_{1/2}$) for gastric emptying were obtained before the development of diabetes. After the onset of diabetes, gastric emptying was measured weekly. After the development of delayed gastric emptying, mice were assigned to treatment with vehicle or IL10 (1 or 0.1 μg intraperitoneally, twice a day; GenScript, Piscataway, NJ; or Insight Genomics, Falls Church, VA). We alternated the assignment to treatment based on the development of delayed gastric emptying only and without regard to any metabolic parameters such as blood glucose or MDA levels. Treatment began after 2 consecutive measurements of delayed gastric emptying and continued as 2 doses every day until 2 consecutive normal values for $T_{1/2}$ were obtained or a maximum of 10 weeks after the start of treatment. The duration and frequency of vehicle treatment was matched to the length of IL10 treatment. All mice with delayed gastric emptying also had MDA levels that were significantly greater than the upper limit of the normal range for MDA in diabetic NOD mice (>73 nmol/mL).[7] At the completion of the study, mice were killed by carbon dioxide exposure followed by cervical dislocation. Whole stomachs were cut along the lesser curvature and the mucosa was removed. Electrical recordings and immunohistochemical studies then were performed on the tissues. The experimental protocol is outlined in Figure 1A.

Electrophysiological Recordings From the Gastric Smooth Muscle

Smooth muscle membrane potential and electrical slow waves were recorded from the circular muscle of every tissue from the treated mice at 12 defined regions distributed from the proximal body to distal antrum (Figure 1B). Sharp glass microelectrodes filled with 3 mol/L KCl (input resistances, 40–70 MΩ) were used to record membrane potential and electrical slow wave. The locations of the recording sites were documented on a digital image, after which the tissue was fixed in the recording dish (Figure 1B). Electrical slow-wave events were analyzed using Clampfit (Molecular Devices, LLC, Sunnyvale, CA). An analysis was performed on recordings longer than 2 minutes in duration in which at least 12 slow-wave events were observed as follows. Slow-wave events from stable recordings were identified using the "template search" event discriminator function in Clampfit. For each trace, a template was derived

A

B
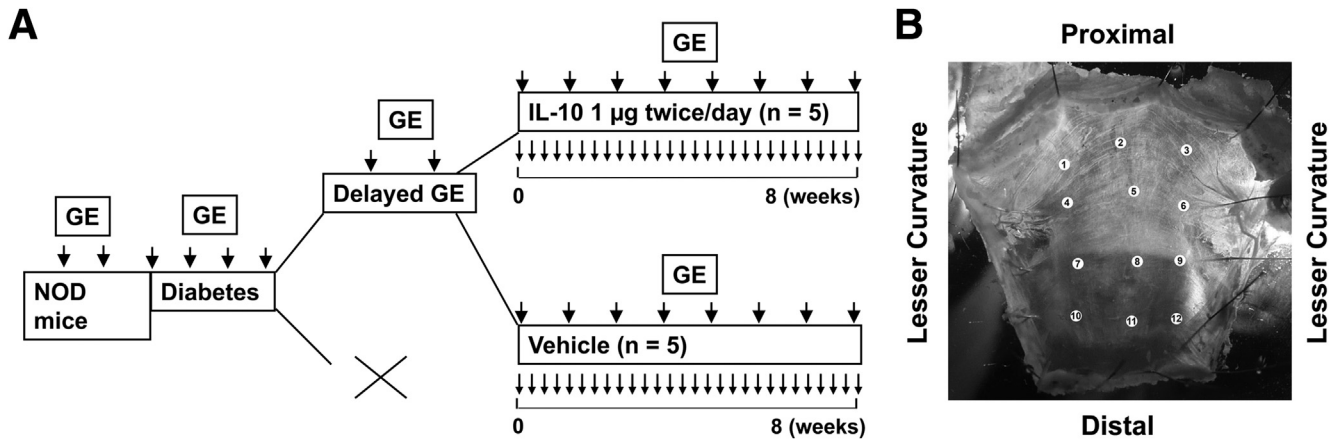
Figure 1. (A) Experimental design. Gastric emptying (GE) is indicated by *larger arrows*, treatment is indicated by *small arrows*. (*B*) Location of electrical recording and image collection sites.

from a typical event. All the events then automatically were fit using the established template, and each event was confirmed by the user for goodness-of-fit. Automated fitting allowed quantification of the baseline membrane potential, peak amplitude, and interevent interval. The interevent interval represents the frequency of the pacemaking depolarization. Averages and variances were obtained for each recording from each area.

Immunohistochemistry

After completion of the electrical recordings, the intact tissues from each mouse were fixed in acetone and doubly labeled for Kit and HO1. Antibodies used were a rabbit polyclonal anti-HO1 antibody (Stressgen Biotech Corp, Victoria, BC, Canada) and rat monoclonal anti-Kit antibody (ACK2; eBioscience, San Diego, CA). The tissue was washed 3 times in 0.1 mol/L phosphate-buffered saline (PBS), and then blocked in 10% normal donkey serum (NDS) in PBS and 0.3% Triton overnight at 4°C. The Kit antibody (final concentration, 1.7 μg/mL) was applied by incubation in 5% NDS/PBS/0.3% Triton X-100 (Thermo Fisher, Waltham MA) for 2 days at 4°C. After the tissue was fixed again in 4% paraformaldehyde in 0.1 mol/L phosphate buffer and washed 3 times in PBS, anti-HO1 antibody (final concentration, 0.125 μg/mL; Stressgen Biotech Corp) in 5% NDS/PBS/0.3% Triton was applied overnight at 4°C. After rinsing in PBS, donkey anti-rabbit fluorescein isothiocyanate (final concentration, 3 μg/mL; Chemicon, Temecula, CA) and donkey anti-rat Cy3 (final concentration, 3 μg/mL; Chemicon) were added in 2.5% NDS/PBS/0.3% Triton and incubated overnight at 4°C in the dark. After rinsing in PBS, nuclei in the tissue were stained by incubating the tissue for 30 minutes at 4°C with 0.3 μmol/L 4',6-diamidino-2-phenylindole dihydrochloride (Molecular Probes, Inc, Eugene, OR) in water.

To identify the HO1-positive cells that had macrophage-like morphology in the muscularis propria of diabetic mice treated with IL10, we treated 2 diabetic mice with 1 μg IL10 twice daily for 1 week. These mice were B6;C3Fe wild-type mice that were made diabetic by treatment with 160 mg/kg streptozotocin as described previously.[24] Treatment with

IL10 was started after 10 weeks of diabetes. The mice had normal gastric emptying. After killing the mice, we immunolabeled the gastric muscularis propria as a whole-mount preparation with the pan-macrophage marker F4/80, the M2 macrophage marker CD206, and HO1 as previously reported.[8] Briefly, tissues were incubated in F4/80 rat anti-mouse antibody (0.4 μg/mL; Thermo Fisher, Waltham, MA) in Ca^{2+}-containing, HEPES-buffered physiologic salt solution (135 mmol/L NaCl, 5 mmol/L KCl, 2 mmol/L $CaCl_2$, 1.2 mmol/L $MgCl_2$, 10 mmol/L glucose, and 10 mmol/L HEPES, adjusted to pH 7.4 with Tris) at 37°C for 90 minutes in the dark. The tissue then was fixed in 4% paraformaldehyde in 0.1 mol/L phosphate buffer. After blocking in 10% NDS, 0.1 mol/L PBS, 0.3% Triton overnight at 4°C, rabbit anti-HO1 (0.125 μg/mL) and goat anti-CD206 (0.5 μg/mL; Santa Cruz Biotech, Santa Cruz, CA) antibodies were applied by incubation in 5% NDS/1× PBS/0.3% Triton overnight at 4°C. After rinsing in PBS, donkey anti-rabbit cy3 (0.5 μg/mL; Jackson ImmunoResearch, West Grove, PA) and donkey anti-goat cy5 (0.5 μg/mL; Jackson ImmunoResearch), both in 2.5% NDS/1× PBS/0.3% Triton were added overnight at 4°C in the dark. The tissues then were washed in PBS and water and the nuclei in the tissue were stained by incubating for 30 minutes at 4°C with 0.3 μmol/L 4',6-diamidino-2-phenylindole dihydrochloride in water and mounted for viewing.

Assessment of Nitric Oxide Synthase Expression in Myenteric Neurons

Nitric oxide synthase expression was determined by reduced nicotinamide adenine dinucleotide phosphate (NADPH) diaphorase histochemistry as previously reported.[25] Tissues, fixed in acetone and paraformaldehyde, were washed 5 times over 30 minutes in 1× PBS and then pinned on Sylgard, Dow Corning, Midland MI in a small Petri dish. Tissues then were washed 2 times in 100 mmol/L TrisCl for 5 minutes and permeabilized in 100 mmol/L TrisCl/0.3% Triton X-100. The labeling solution contained 0.2 mg/mL nitroblue tetrazolium and 1 mg/mL NADPH dissolved in 100 mmol/L TrisCl/0.3% Triton X-100 and was incubated with the tissue at 37°C until the reaction was

complete. The reaction was stopped by washing in 100 mmol/L TrisCl/0.3% Triton X-100. Tissues then were mounted for examination at 20× magnification on an upright microscope and counting of positively labeled cells.

Assessment and Quantification of Kit and HO1 Immunoreactivity

Tissues were examined with a confocal microscope using a 20× (numerical aperture, 0.95) XLUMPlanFl objective (Olympus, Tokyo, Japan) in Fluoview (Olympus) at a resolution of $0.994 \times 0.994 \times 1.13$ μm (X × Y × Z). Stacks of images across the full thickness of the muscles were collected from the documented electrical recording sites. To assess labeling across the whole stomach, tissues were examined with an Olympus IX70 microscope by 2 investigators blind to the tissue source. For quantification of the labeling specifically at the electrical recording sites, all of the confocal image stacks (120 images for each immunolabel) were flattened into projections using the FV10-ASW Viewer (Olympus), assigned a random number, and uploaded onto a digital album in random order. The images then were assessed using the same parameters as used for the whole tissue by 2 investigators blind to the tissue source. The images were scored on a 10-cm visual analogue scale for network density, connectivity, and structural preservation. The scores for each image then were averaged and the code was broken to find which image belonged to which field and animal.

Quantification of Connectivity in the Confocal Images of Kit Immunoreactivity

The absolute volumes of Kit-positive immunoreactivity in 4 fields from 2 areas in each tissue where electrical abnormalities were most evident in the vehicle-treated mice were obtained by volume rendering and 3-dimensional reconstruction from confocal image stacks of ICC across the full thickness of the muscle using Analyze (Mayo Foundation, Rochester, MN) as previously described.[26] The reconstructed Kit-positive 3-dimensional structures from each field were subjected to a morphologic $3 \times 3 \times 3$ opening operation. This deleted any region of the structures that did not contain a $3 \times 3 \times 3$ voxel (12.86 μm^3) cube, thereby breaking up larger tenuously connected structures into 2 or more smaller structures. After opening, the remaining connected structures larger than 100 voxels (143 μm^3) were counted. A larger number of such structures within similar total volumes indicated reduced connectivity of the total volume.

Statistics were performed with Prism (GraphPad, La Jolla, CA) using the appropriate tests as described in the Results section. All authors had access to the study data and have reviewed and approved the final manuscript.

Results

### Blood Glucose and Oxidative Stress Levels in Diabetic Mice

Mice used for this study developed diabetes at 19.6 ± 1.6 weeks (mean ± SEM, n = 10 mice), and remained diabetic throughout the study. Thirty percent of diabetic mice developed delayed gastric emptying at a mean of 5.4 ± 0.5 weeks (mean ± SEM, n = 10 mice) after the onset of diabetes. This is consistent with previous reports.[7] Animals with delayed gastric emptying were enrolled consecutively until 10 mice completed the study. Five mice received vehicle and 5 mice received IL10. There were no significant differences in blood glucose levels for the mice whether treated with vehicle or IL10 at any point during the progression of the study and diabetic mice with delayed gastric emptying did not have significantly different blood glucose levels compared with diabetic mice with normal gastric emptying (Figure 2A). Vehicle and IL10-treated mice received similar amounts of insulin during the study (3.4 ± 1.80 IU/day vs 2.6 ± 0.98 IU/day, respectively, mean ± SEM; n = 5 mice; $P = .67$, t test).

Systemic oxidative stress was measured using plasma MDA levels. Nondiabetic mice had low levels of MDA (6.0 ± 0.6 and 6.0 ± 0.5 nmol/mL for mice assigned to vehicle and IL10, respectively, mean ± SEM; n = 5 in each group) (Figure 2B). After the development of diabetes but while gastric emptying remained normal, MDA levels were not significantly different between the mice assigned to the 2 treatments (41 ± 16.3 and 30 ± 3.7 nmol/mL for mice assigned to vehicle and IL10, respectively, mean ± SEM; n = 5 in each group) (Figure 2B). At the onset of delayed gastric emptying, MDA levels were increased further above the previously established normal range for diabetic NOD mice with normal gastric emptying (normal mean, 53.05; range, 28–73 nmol/mL; n = 19 mice),[7] in both groups of mice (129 ± 28.9 and 226 ± 16.8 nmol/mL, mean ± SEM, vehicle and IL10, respectively). These levels at the onset of delayed gastric emptying were higher than the 73 nmol/mL threshold previously found to be associated with delayed gastric emptying in diabetic NOD mice.[7] In mice treated with IL10, MDA levels decreased to the levels (56 ± 9.9 nmol/mL, mean ± SEM) typical for diabetic NOD mice with normal gastric emptying whereas MDA levels in the vehicle-treated mice remained greater than the upper limit of this range (Figure 2B) (221 ± 37.2 nmol/mL, mean ± SEM). These values were higher than those before the development of delayed gastric emptying and higher than the levels in mice treated with IL10 (Figure 2B).

Gastric Emptying in Diabetic Mice After IL10 Treatment

Gastric emptying values are shown in Figure 2C. Before the development of diabetes, gastric emptying values were in the normal range.[11] $T_{1/2}$ values were 97 ± 7.1 and 98 ± 6.0 minutes for mice assigned to vehicle and IL10, respectively (mean ± SEM; n = 5 in each group) (Figure 2C). The gastric emptying values in diabetic mice after development of a delay were not different between groups ($T_{1/2} = 174 \pm 13.9$ min for vehicle, 183 ± 19.4 min for IL10, mean ± SEM; n = 5) (Figure 2C). In mice that were treated with IL10, gastric emptying returned to normal in all animals after 8.8 ± 1.9 weeks ($T_{1/2} = 106 \pm 3.4$ min, mean ± SEM; n = 5) (Figure 2C), whereas mice treated for the same period with vehicle continued to have delayed gastric emptying ($T_{1/2} = 159 \pm 9.5$ min, mean ± SEM; n = 5) (Figure 2C).
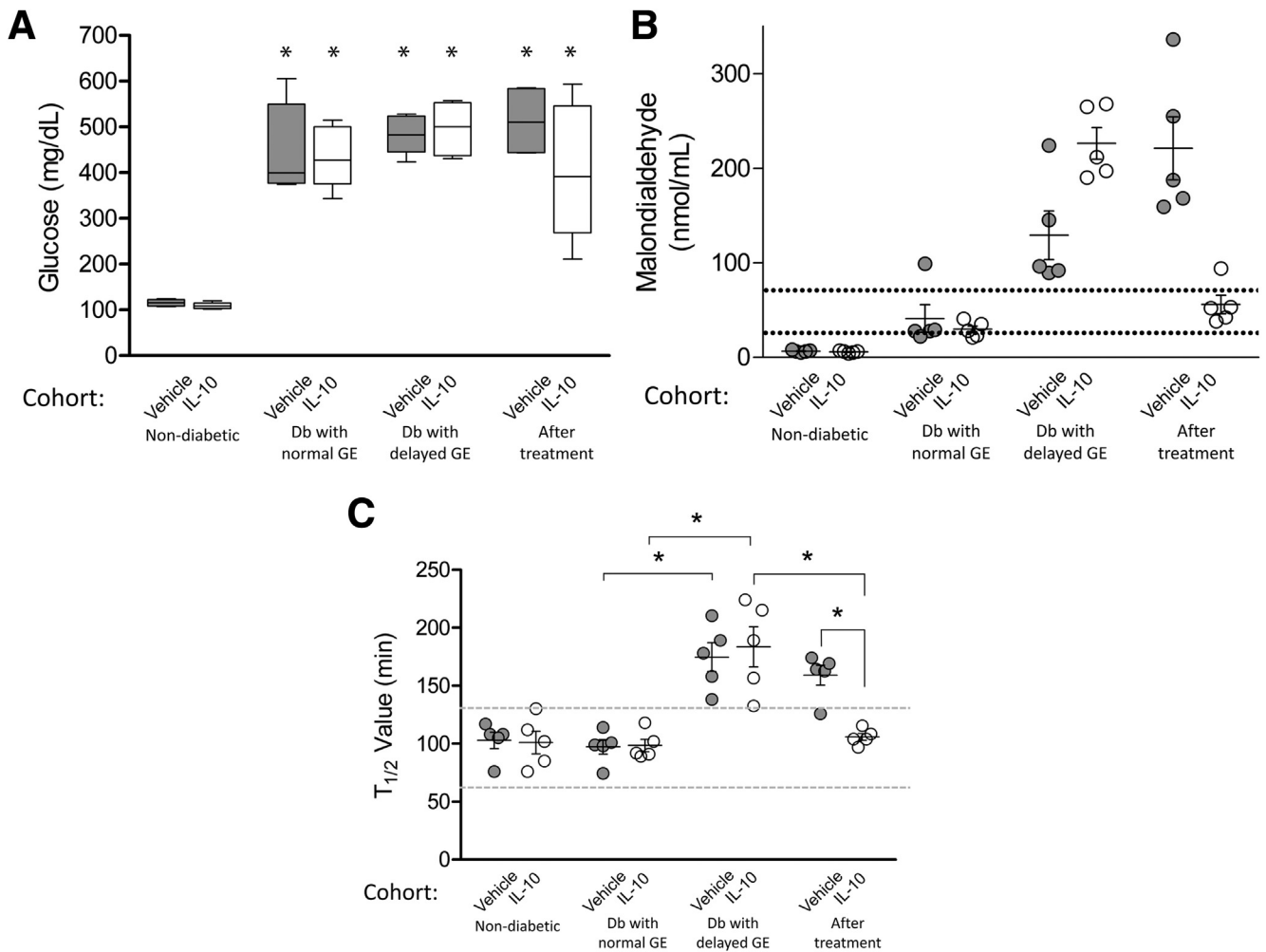
Figure 2. Effects of IL10 treatment. (A) Glucose levels (*bars*, medians with interquartile range; *whiskers*, 5th/95th percentiles). *Higher glucose levels for diabetic vs nondiabetic mice (n = 5; 2-way analysis of variance with Bonferroni post-test). (B) Malondialdehyde levels were associated significantly with delayed gastric emptying and response to IL10 treatment but not diabetes. *Circles*, values for each mouse; *whiskers*, means ± SE; *dotted lines*, 5th/95th percentile of MDA levels in diabetic NOD mice with normal gastric emptying. (C) Gastric emptying. *Circles*, data of each mouse; *whiskers*, means ± SE; *dotted lines*, 5th/95th percentile of $T_{1/2}$ values in nondiabetic mice. *$P < .05$ (n = 5; 1-way analysis of variance with the Tukey post-test). Db, diabetic; GE, gastric emptying.

These data support the conclusion that IL10 can reverse delayed gastric emptying over an 8-week period with no effects on blood glucose levels. We next determined the effect of IL10 on electrical activity.

Electrical Activity After Treatment With IL10

Stable electrical recordings were made from 12 areas in the corpus and antrum of all diabetic mice with delayed gastric emptying that then completed the study of the effects of treatment with vehicle or IL10 on gastric emptying (120 regions in total). In regions where slow waves could be detected (116 areas), there were differences in the properties of the electrical activity between vehicle- and IL10-treated mice. Quiescent areas were all in the proximal body (areas 1–3), close to the fundus, an area where slow waves usually are not detected. The quiescent areas were found in 2 tissues from both vehicle- and IL10-treated mice.

Peak amplitudes of the slow waves recorded in the distal region (areas 10–12) of the IL10-treated mice did not vary as much as the peak amplitudes of slow waves in the same regions from vehicle-treated mice. In the more proximal regions of the stomach, irregularities in the slow waves from 3 of 5 vehicle-treated animals also were observed, but this was not observed for any IL10-treated mice. In all tissues from vehicle-treated mice, an irregular slow-wave pattern was recorded in the distal antrum (Figure 3A), whereas the slow-wave activity for the IL10-treated animals did not show these irregularities in the equivalent areas of the distal antrum (Figure 3B). This reduction in the variability of the slow wave in the antrum after IL10 treatment was confirmed by quantifying the peak amplitude of the slow waves. We averaged the amplitudes of all events in each recording, both low- and high-amplitude events, but found that there was no difference in the actual amplitude of the slow waves by comparing either individual regions or
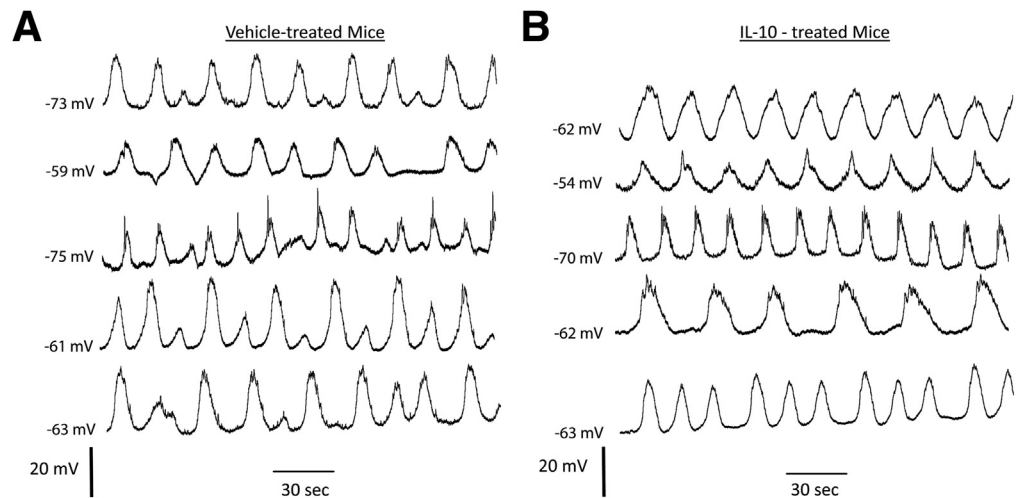
Figure 3. Electrical activity. Slow-wave activity in the distal antrum of all (A) vehicle-treated and (B) IL10-treated mice. Note the variations in peak amplitude of the slow waves in the vehicle-treated mice that are absent in the IL10-treated mice.
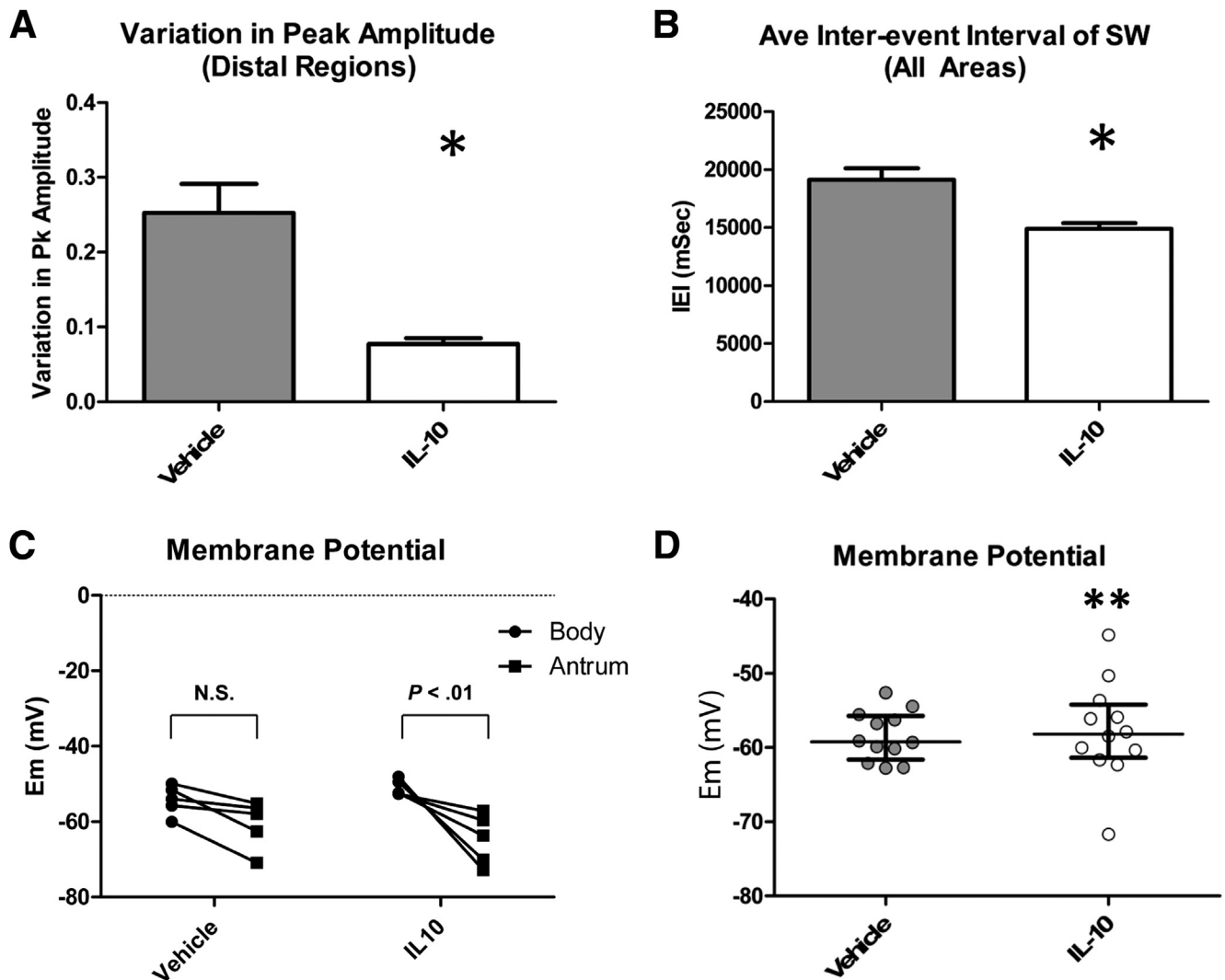
averages of the observations at all regions, but there was significantly more variation in the amplitude for the most distal regions (Figure 4A) ($P < .05$, unpaired t test; n = 5). The events recorded from IL10-treated mice also had significantly higher frequencies (4.05 ± 0.34 cycles/min) with, on average, a 22% shorter peak-to-peak interevent interval compared with vehicle-treated mice (3.18 ± 0.4 cycles/min; $P = .0052$, unpaired t test; n = 5) (Figure 4B). A faster frequency also was detected in tissues from IL10-treated mice by comparing the interevent intervals at every individual recording location ($P < .05$, Wilcoxon matched-pairs test). A smooth muscle membrane potential gradient exists between the proximal and distal stomach in dogs.[27] In healthy wild-type mice, the smooth muscle membrane potential in the antrum is reported to be hyperpolarized relative to the fundus,[28] and the values are similar to those found in the equivalent areas of the canine stomach.[27] The membrane potential difference between the proximal and distal areas of the stomach was not significant in tissues from the diabetic with delayed emptying, vehicle-treated mice (corpus 1–3, Membrane potential, (E_m) = -54.2 ± 1.76 vs antrum 7–9, antrum, -60.6 ± 2.87 mV, NS, n = 5), although there was a significant membrane potential difference in tissues from IL10-treated mice, with proximal regions (areas 1–3, corpus, E_m = -51.0 ± 0.96 mV, mean ± SEM) significantly more depolarized than distal regions (areas 7–9, antrum, E_m = -64.7 ± 3.00 mV, mean ± SEM; $P < .01$, 2-way analysis of variance with Bonferroni post-test; n = 5) (Figure 4C). In addition, the variation in the membrane potential values across the whole tissue was significantly greater in the IL10-treated mice compared with the vehicle-treated mice (Figure 4D) ($P = .03$, F-test).

Changes in Kit-Positive ICC, HO1-Positive Cells, and Neuronal Nitric Oxide Synthase Activity After IL10 Treatment

We next determined if the IL10-induced changes in gastric emptying and electrical activity were accompanied by cellular changes. All of the tissues used for electrophysiology were processed as whole mounts and immunolabeled using antibodies to HO1 and Kit. The whole tissues were examined at low power under an epifluorescence microscope. High-resolution confocal images also were collected from the electrical recording sites as identified by careful mapping. Overall, there was a clear difference between the tissues from IL10- and vehicle-treated mice (Figure 5A and B). Blind scoring showed that expression of HO1 protein was significantly higher in tissue from IL10- compared with vehicle-treated mice (Figure 5C), and that tissues from IL10-treated mice had more HO1-positive cells than tissues from vehicle-treated mice. HO1-positive cells were distributed unevenly across the tissue with patches of positively labeled cells in some areas but not others (Figure 5A and B). Most of the labeled cells had the macrophage-like morphology (Figure 5D) that we previously reported for CD206-positive, F4/80-positive cells in the gastric muscularis propria of diabetic NOD mice with normal gastric emptying and were likely M2 macrophages.[7] HO1 protein expression also was up-regulated in some myenteric ganglia (Figure 5D) from 2 of 5 IL10-treated mice. To test whether the HO1-positive, macrophage-like cells were M2 macrophages, we triply labeled gastric body muscularis propria from 2 diabetic mice that had been treated with IL10 for 2 weeks. As shown in Figure 5E, the majority of HO1-positive cells with macrophage-like morphology expressed not only the panmacrophage marker F4/80 but also the M2 macrophage marker CD206. We examined nitric oxide synthase activity in the myenteric plexuses of vehicle- and IL10-treated tissues by counting NADPH-diaphorase–positive neurons. There was no difference in the number of labeled neurons (vehicle, 46 ± 11; IL10, 42.8 ± 5.9 neurons/field; NS, unpaired t test) (Figure 6).
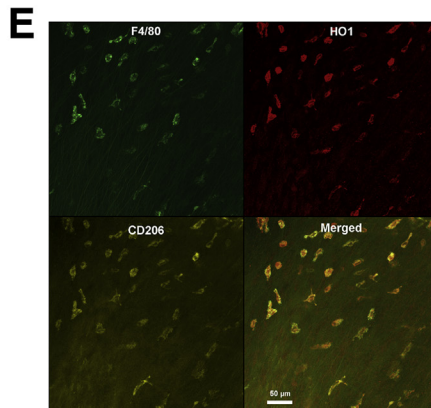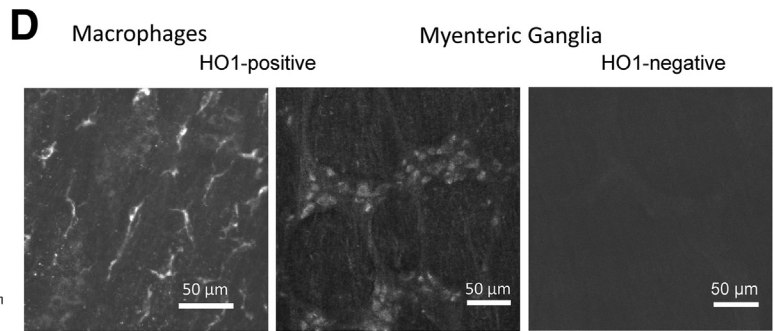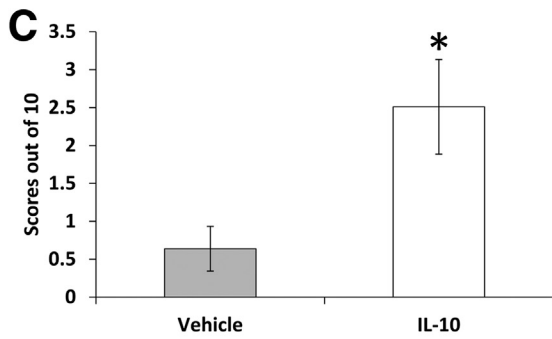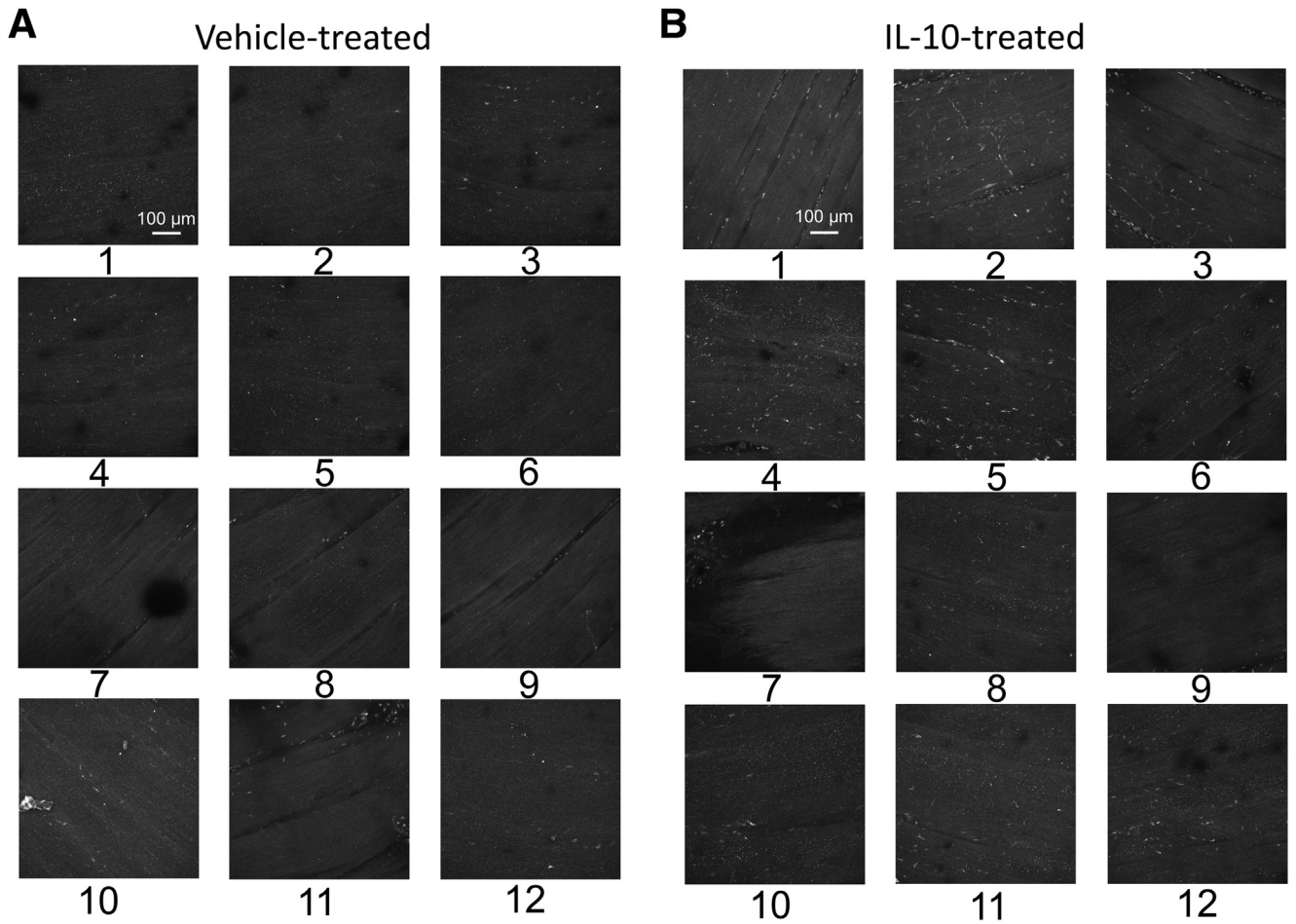
ICC networks, as identified by Kit immunoreactivity, were significantly different between IL10- and vehicle-treated groups. Quantification of the differences at the whole-tissue level was performed by collecting high-resolution confocal images at the location of all the electrical recording sites (120 images) (Figure 7A and B), and
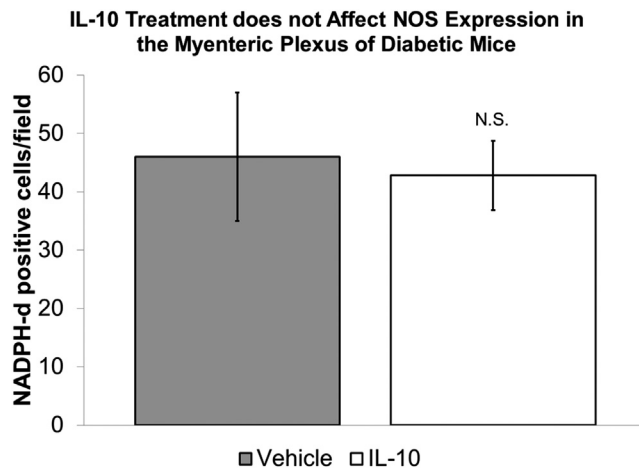
A

Variation in Peak Amplitude (Distal Regions)

B

Ave Inter-event Interval of SW (All Areas)

C

Membrane Potential

D

Membrane Potential

Figure 4. Electrical activity. Response to IL10 treatment. (*A*) Variability of peak amplitudes in the distal stomach (regions 7–12). Means ± SEM. *$P < .05$, one-way analysis of variance with Bonferroni correction; n = 5. (*B*) Quantification of the interevent intervals (IEIs) for slow waves from all areas of all mice. Means ± SEM; n = 5. *$P < .05$, unpaired *t* test. (*C*) Resting membrane potential in the corpus (regions 1–3) and antrum (regions 7–9) of vehicle- and IL10-treated diabetic mice. Each *point* represents the membrane potential for each mouse. Statistical differences were determined by repeated measures 2-way analysis of variance with a Bonferroni post-test; N = 5 mice. (*D*) Resting membrane potential. Note the variance in the membrane potential across tissues was different. **$P = .03$, F-test; means for 12 recording sites; n = 5 mice. *Whiskers*, medians–interquartile range. Pk, peak.

scoring of network density in a blind fashion by 2 independent investigators on a 10-cm scale. The blinded observers reported that tissues that subsequently were identified as vehicle-treated had clear regions where ICC networks were depleted and, in other areas, where ICC were present, the networks were scored as more disorganized. In tissues subsequently identified from IL10-treated mice, the density of ICC networks was more even across the tissue and the networks were scored as more organized and more evenly labeled for Kit. These scores found that ICC in IL10-treated mice had significantly higher ICC densities across the whole tissue compared with vehicle-treated mice (Figure 7*C*).We separately investigated whether local ICC network changes corresponded with abnormalities in electrical slow waves by selecting 2 recording locations from

each tissue, collecting high-resolution images and determining Kit-positive ICC volume and connectivity at those recording locations in the proximal and distal antrum from both IL10- and vehicle-treated mice. The investigator performing this work was blind to the source of the images that were reconstructed. The volume of the Kit-positive structures in these images was not different between ICC networks from the 2 groups of mice in either the distal antrum where the slow-wave changes were most prominent or in the proximal antrum where they were less common (Figure 7*D*) (n = 5 mice; $P > .05$, unpaired *t* test). However, an analysis of the count of connected structures after morphologic opening showed that ICC networks from IL10-treated mice were significantly more connected than vehicle-treated networks (Figure 7*E*). The algorithm used

A Vehicle-treated

B IL-10-treated

C

D Macrophages Myenteric Ganglia
HO1-positive   HO1-negative

E

IL-10 Treatment does not Affect NOS Expression in the Myenteric Plexus of Diabetic Mice

Figure 6. NADPH-diaphorase activity. Quantification of neurons in the myenteric plexus from diabetic NOD mice with delayed gastric emptying treated with vehicle or 1 μg IL10 twice a day. Positively labeled neurons were counted from 7 high-power fields using a 20× objective from each tissue. A minimum of 174 neurons were counted from each tissue. There was no significant difference in the number of positively labeled neurons between the 2 groups (means ± SEM, *t* test).

for this analysis examines the impact of eroding the map equally across the volume and examining the size and number of the resulting fragments. In vehicle-treated mice, the network breaks up into more objects with the same processing compared with the samples from IL10-treated mice (Figure 7E) (n = 75 areas; $P = .026$, unpaired *t* test). These data quantify the greater organization of the ICC networks in IL10-treated mice. To illustrate this difference, we show examples of the largest connected Kit-positive ICC networks in 2 fields in the distal antrum that were segmented from a vehicle-treated and an IL10-treated mouse (Figure 7F). These selections show a higher level of connectivity of the ICC networks in the IL10-treated mice.

Effect on Gastric Emptying of Treatment With a Lower Dose of IL10

We also tested a 10-fold lower dose of IL10 in a separate cohort of diabetic NOD mice with delayed emptying. After onset of delay, mice were treated with 100 ng IL10 twice a day. One mouse was removed from the study because glucose levels decreased to prediabetic levels. Gastric emptying returned to normal values in all 4 remaining mice (Figure 8) ($T_{1/2}$ predelay, 87 ± 8; pre-IL10 treatment, 196 ± 11; and post-IL10 treatment, 110 ± 8 min; $P < .05$ before vs after IL10) in a mean of 4.8 weeks, which was not a

significantly different time to respond than found for the higher 1-μg dose of IL10.

Discussion

This study shows that treatment with IL10 for delayed gastric emptying in diabetic mice restores gastric emptying to normal. This effect was accompanied by reduced levels of oxidative stress indicated by lower levels of the systemic lipid peroxidation marker, malondialdehyde, up-regulation of HO1 expression in the muscularis propria, higher integrity of Kit-positive ICC networks, and by normalization of electrical slow wave activity.

Mice received 0.1 or 1 μg IL10 twice a day, which is equivalent to 5–50 μg/kg twice a day in human beings.[29] Animals receiving the high dose of IL10 were not more sick than vehicle-treated mice, even though the mice under study had increased blood glucose levels and gastroparesis. This is consistent with the experience with IL10 in human beings, in whom treatment was shown to be safe and well tolerated at doses up to 25 μg/kg, with a few complications in subjects receiving 50–100 μg/kg.[29,30]

There was no consistently beneficial clinical response when IL10 was tested as a treatment for inflammatory bowel disease, rheumatoid arthritis, or psoriasis,[31] and in trials studying the effectiveness of IL10 in treatment of Crohn's disease, 20 μg/kg resulted in increased expression of blood markers for inflammation.[32] The side effects observed, and lack of response to treatment, has resulted in withdrawal of many patients treated with IL10 for Crohn's disease.[33] Our studies indicate that diabetic delayed gastric emptying in mice is not the result of an adaptive immune response but is owing to a particular, macrophage-dependent mechanism,[8] which may explain why IL10 was effective in treating delayed emptying. Interestingly, IL10 was very effective in preventing postoperative ileus in mice,[16] also an innate response and supporting the concept that IL10 has more promise in innate immune rather than adaptive immune disorders. This study tested IL10 as a treatment for delayed gastric emptying and our study was not designed to find out if continued treatment is necessary to sustain the benefit. Further studies are necessary to determine the optimal dose and means of delivery of IL10 to treat gastroparesis most effectively. One possibility includes delivering IL10 orally using IL10-releasing lactococci, as was shown recently in another study.[34]

We also showed that IL10 was effective in normalizing disrupted slow-wave activity. Disrupted slow-wave activity was reported previously in studies that compared the electrical properties of the gastric muscularis propria in NOD mice with long-standing and uncontrolled diabetes with activity in nondiabetic mice.[9] Irregular electrical

Figure 5. (*See previous page*). HO1 expression. Image stacks of HO1 immunoreactivity in (*A*) vehicle and (*B*) IL10 mice. Numbers indicate regions. (*C*) Scores for HO1 immunoreactivity. Means ± SEM; n = 5; *$P < .01$, *t* test. (*D*) HO1-positive macrophages (*left*) and neurons in a myenteric ganglion (*middle*) from the gastric body of IL10-treated mouse. *Right*: a ganglion from an IL10-treated mouse in which HO1 was not detected in the neurons. (*E*) Image stacks of F4/80, HO1, and CD206 immunoreactivity in the muscularis propria of a diabetic mouse treated with IL10. Data are representative of immunolabeling in 2 different mice.
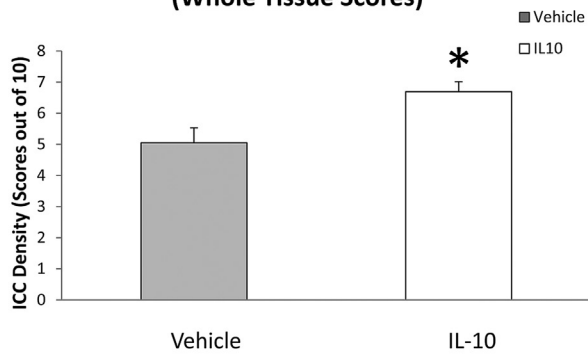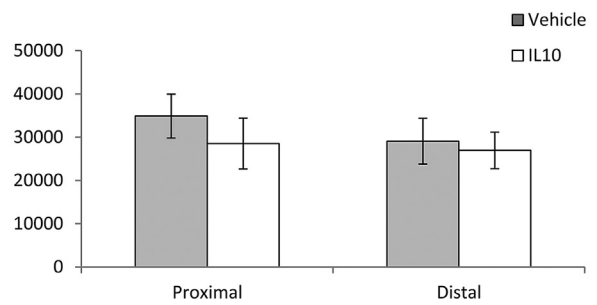
A Vehicle-treated Mouse
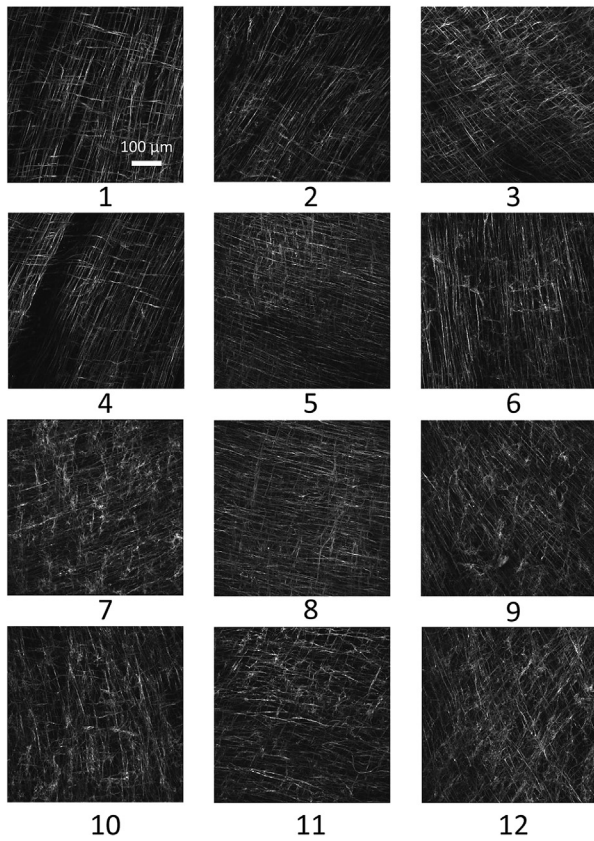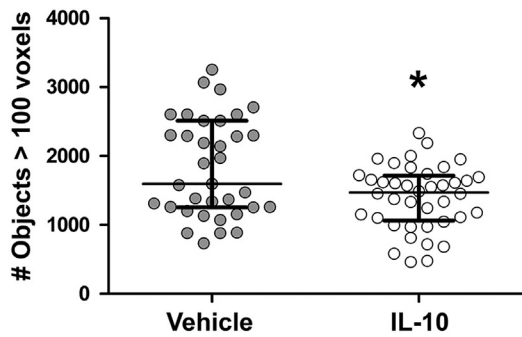

B IL-10-treated Mouse
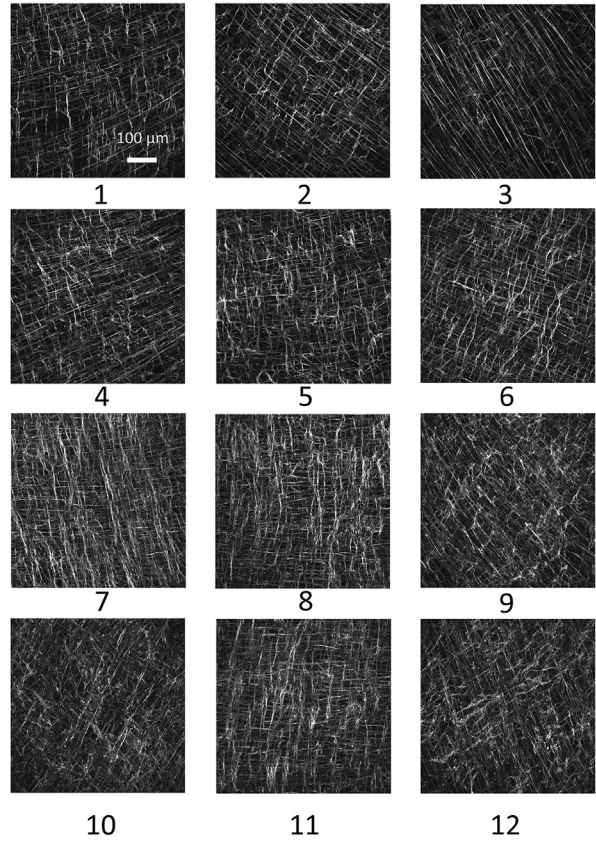
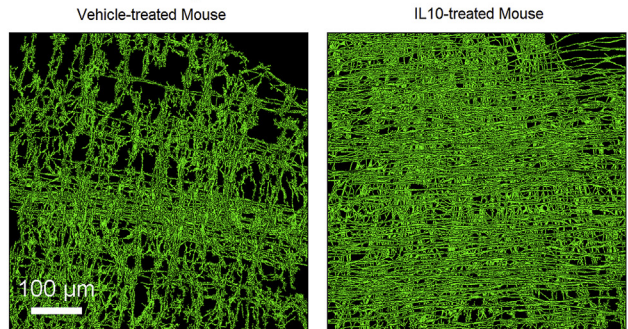**C** Overall Density of ICC (Whole Tissue Scores)

D Kit Volume in Antral Regions (Voxels per Slice)

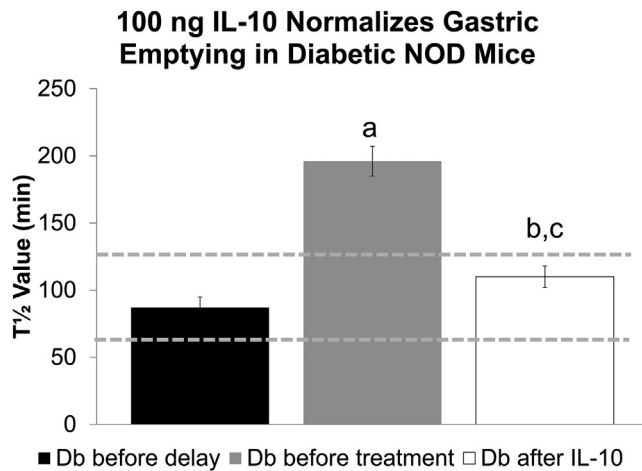**E** Number of Connected Objects

F Largest Connected Object in Image 3D Volume Rendered Image

100 ng IL-10 Normalizes Gastric Emptying in Diabetic NOD Mice

Figure 8. *A low dose of IL10 (100 ng) also reversed delayed gastric emptying in diabetic NOD mice.* Data are the mean $T_{1/2}$ values for gastric emptying $\pm$ SEM. $P < .001$, 1 way analysis of variance. $P < .05$ vs Db before delay (*a*); $P < .05$ vs Db before treatment (*b*); and not significantly different vs Db before delay (*c*). Db, diabetic.

rhythmicity in the human stomach also has been reported in diabetic gastroparesis.[21–23] In diabetic rodents, other studies have reported observations similar to those that we found in vehicle-treated mice with delayed emptying.[9,20] Both groups observed more severe changes in slow-wave activity than we did, but the pattern of changes was the same. Ordog et al[9] reported diminished slow-wave frequencies and amplitudes in cells that had electrical activity, although a majority of cells in the distal stomach (81%) showed no slow wave. Other investigators have reported an absence of slow waves in 13 of 19 preparations from diabetic rats with irregular and small events in preparations in which activity was detected.[20] The disadvantage of these previous studies was that they could not do what we did for this report, in which we examined the electrical properties and cellular pathology of the tissues from each mouse, knowing the history of the gastric emptying status of that mouse. All of our mice received low doses of insulin to maintain blood glucose levels at 500–600 mg/dL, so they were not subject to severe ketoacidosis and could be maintained alive for longer than animals that did not receive insulin. This insulin treatment may account for the more modest abnormalities in slow-wave properties from our vehicle-treated animals compared with previous reports.[9,20]

The intrinsic pacing of the electrical slow wave in the stomachs of dogs, pigs, and human beings has been shown, using multi-electrode recordings, to be driven by a region close to the greater curvature in the proximal corpus,[35–37]

and tissue dissection studies have indicated that this likely also is true for mouse stomach.[38] This pacemaker region corresponds to region 5 (proximal corpus) in our experiments, and our observations suggest that IL10 treatment results in better coupling of the pacemaker in the corpus to antral ICC. The immunohistochemical data showing that the vehicle-treated mice have disrupted ICC networks and IL10-treated mice have more even, and better-connected, ICC networks across the whole tissue, support inefficient coupling of the pacemaker in the corpus to other parts of the tissue in vehicle-treated mice that continue to have delayed gastric emptying. Alternatively, abnormal slow waves in the distal antrum of vehicle-treated mice may reflect an accumulation of electrical defects as the slow wave propagates from the corpus to antrum through the disrupted ICC networks. Our previous studies have reported that Kit protein expression by immunoblotting is low in diabetic mice with delayed gastric emptying, high in diabetic mice with normal gastric emptying, and high in mice treated to restore gastric emptying to normal.[7,8,39] Because we observed whole tissue changes to ICC networks but no direct correlation between the uneven slow-wave activity and loss of ICC at the level of the recording sites, we conclude that the key improvement in ICC networks was network integrity. Differences in Kit protein levels might be owing partly to the brighter Kit immunoreactivity in the tissues from IL10-treated mice.

The variable that was most affected by IL10 treatment was the degree of variability in the electrical slow-wave amplitudes. IL10 reduced peak-to-peak variability by more than 50% (see Figure 4*A* for quantification). These differences in peak-to-peak height are unusual and are predicted to disrupt coordination and force of contractility in the distal stomach regions where the abnormalities were most prominent. In human beings with severe symptoms of diabetic gastroparesis and delayed gastric emptying, the electrogastrogram recordings showed a high degree of variability consistent with disorganized pacemaking activity.[21–23] This variability was normalized after successful treatment.[21] It is difficult to correlate the magnitude of the improvement in electrical activity necessary for treating gastroparesis in human beings compared with our studies in mice because the extracellular human electrogastrogram and the mouse intracellular slow waves are 2 different readouts of associated phenomena. However, the observations are congruent in that disorganization and variability in electrical activity in the signal directly correlates with impaired gastric emptying. Irregular slow-wave activity may emerge in the distal stomach as a cumulative effect of ICC defects proximal to the site of the recorded electrical defect. The presence of a difference in the resting membrane

---

Figure 7. (*See previous page*). **ICC networks.** Image stacks from (*A*) vehicle and (*B*) IL10 mice. (*C*) Network density scores. Means $\pm$ SD of scores for all fields; n = 5; *$P < .05$, *t* test. (*D*) Network volume from recording sites in antrum. (*E*) Count of independent connected structures after morphologic opening in reconstructed images. Data are for 75 fields from 5 mice in each group. *$P = .026$, *t* test. (*F*) Three-dimensional (3D) volume-rendered bitmap of the largest connected Kit-positive ICC networks in 2 fields with similar total Kit volumes. Note that most of the Kit-positive structures in the field from the IL10-treated mouse are connected into a single object.

potential from proximal to distal regions of the stomach in IL10-treated mice also may reflect improved function of ICC networks in mice with normal emptying. ICC have been shown to regulate membrane potential and by doing so to act as a rheostat, setting the local efficiency of excitation-contractility coupling.[28]

Treatment with IL10 resulted in increased HO1 expression in macrophage-like cells and changes to ICC networks. It is likely that these macrophage-like cells are M2, CD206-positive macrophages, but we cannot be certain because we did not directly determine the CD206 or F4/80 expression of the HO1-positive cells in the diabetic mice with delayed gastric emptying that were treated successfully with IL10. The likelihood that the macrophage-like cells are M2, CD206-positive macrophages is based on the findings that HO1 expression was identified in CD206-positive, F4/80-positive macrophages but not other cell types in diabetic mice with baseline normal gastric emptying that were treated with IL10. Furthermore, we have not previously seen HO1 expression in CD206-negative, gastric muscularis propria macrophages, and HO1 expression is very low in gastric muscularis propria in nondiabetic mice or diabetic mice with delayed gastric emptying.[7,8] The mechanism for the response to IL10 may be owing to intrinsic cytoprotective properties of M2-macrophages[40] or owing to suppression of proinflammatory M1 macrophages.[19] Up-regulation of CO production owing to increased expression of HO1 also may be key because we showed that CO alone is sufficient to normalize gastric emptying,[39] and multiple studies have shown HO1 activation in cytoprotective responses to IL10.[17,41] The impact of changing macrophage numbers and phenotype on gastric emptying also may be mediated by other factors that have not yet been identified. Our results also show that IL10 induces HO1 in myenteric ganglia in some mice, which might be a specific response in some diabetic NOD mice to IL10. Changes to MDA values may be a consequence or a mediator of the effect of IL10. We did not power our study to determine how IL10 affects MDA values. MDA values in diabetic mice with delayed gastric emptying were increased and highly variable, as previously observed.[7] We randomly assigned the 10 mice with diabetes and delayed gastric emptying to treatment with IL10 or vehicle. By chance, the mice receiving IL10 had the highest MDA values, however, they still responded with normalization of gastric emptying, despite being sicker than the mice receiving vehicle, which did not reverse the delay in gastric emptying and did not achieve normal MDA values. However, given that the study was not powered to distinguish MDA levels between the groups assigned to vehicle and IL10, we cannot assume a trend because the mice came from a population of animals that was assigned blindly without respect to MDA levels.

We did not observe a restoration of NOS activity as previously reported when we treated delayed gastric emptying in diabetic NOD mice using hemin or CO.[7,39] This was unexpected and requires further confirmation.

The most parsimonious explanation for the cellular response to IL10 is that IL10 induces several molecular pathways that are beneficial to gastric function, including reduced oxidative stress, suppression of proinflammatory cytokines, and activation of cellular repair. In these respects, IL10 may have an advantage over inducing HO1 with hemin or administering CO because, for example, suppression of M1-macrophages is a direct effect of IL10[42] and activation of monocytes by IL10 is not dependent on HO1 activity.[43] The mechanisms for repair to ICC networks also were likely to be owing to an interaction of several processes including reduced oxidative stress, which lowers the levels of toxic products of lipid peroxidation, as well as activation of proliferative and anti–cell death pathways by CO.[14]

In conclusion, these studies suggest that IL10 is a promising therapy for diabetic gastroparesis in human beings because the response to treatment in diabetic NOD mice affects 2 well-defined characteristics of human diabetic gastroparesis. Those features are irregular electrical rhythmicity[21–23] and a correlation between damage to ICC and delayed emptying.[5] There is also reason to propose that modulating macrophage phenotype using IL10 will be effective in human beings because the number of CD206-positive macrophages also correlates with the number of ICC in human beings with diabetic gastroparesis.[12]

References

1. Farrell FJ, Keeffe EB. Diabetic gastroparesis. Dig Dis 1995;13:291–300.
2. Vittal H, Farrugia G, Gomez G, et al. Mechanisms of disease: the pathological basis of gastroparesis–a review of experimental and clinical studies. Nat Clin Pract Gastroenterol Hepatol 2007;4:336–346.
3. Camilleri M, Grover M, Farrugia G. What are the important subsets of gastroparesis? Neurogastroenterol Motil 2012;24:597–603.
4. Camilleri M. Clinical practice. Diabetic gastroparesis. N Engl J Med 2007;356:820–829.
5. Grover M, Bernard CE, Pasricha PJ, et al. Clinical-histological associations in gastroparesis: results from the Gastroparesis Clinical Research Consortium. Neurogastroenterol Motil 2012;24:531–539, e249.
6. Grover M, Farrugia G, Lurken MS, et al. Cellular changes in diabetic and idiopathic gastroparesis. Gastroenterology 2011;140:1575–1585 e8.
7. Choi KM, Gibbons SJ, Nguyen TV, et al. Heme oxygenase-1 protects interstitial cells of Cajal from oxidative stress and reverses diabetic gastroparesis. Gastroenterology 2008;135:2055–2064, 64 e1–2.
8. Choi KM, Kashyap PC, Dutta N, et al. CD206-positive M2 macrophages that express heme oxygenase-1 protect against diabetic gastroparesis in mice. Gastroenterology 2010;138:2399–2409, 409 e1.
9. Ordog T, Takayama I, Cheung WK, et al. Remodeling of networks of interstitial cells of Cajal in a murine model of diabetic gastroparesis. Diabetes 2000;49:1731–1739.
10. Watkins CC, Sawa A, Jaffrey S, et al. Insulin restores neuronal nitric oxide synthase expression and function that is lost in diabetic gastropathy. J Clin Invest 2000;106:373–384.

11. Choi KM, Zhu J, Stoltz GJ, et al. Determination of gastric emptying in nonobese diabetic mice. Am J Physiol Gastrointest Liver Physiol 2007;293:G1039–G1045.

12. **Bernard CE, Gibbons SJ**, Mann IS, et al. Association of low numbers of CD206-positive cells with loss of ICC in the gastric body of patients with diabetic gastroparesis. Neurogastroenterol Motil 2014;26:1275–1284.

13. Bharucha AE, Kulkarni A, Choi KM, et al. First-in-human study demonstrating pharmacological activation of heme oxygenase-1 in humans. Clin Pharmacol Ther 2010; 87:187–190.

14. **Gibbons SJ, Verhulst PJ**, Bharucha A, et al. Review article: carbon monoxide in gastrointestinal physiology and its potential in therapeutics. Aliment Pharmacol Ther 2013;38:689–702.

15. Moore BA, Otterbein LE, Turler A, et al. Inhaled carbon monoxide suppresses the development of postoperative ileus in the murine small intestine. Gastroenterology 2003;124:377–391.

16. Stoffels B, Schmidt J, Nakao A, et al. Role of interleukin 10 in murine postoperative ileus. Gut 2009;58:648–660.

17. Lee TS, Chau LY. Heme oxygenase-1 mediates the anti-inflammatory effect of interleukin-10 in mice. Nat Med 2002;8:240–246.

18. Deng B, Wehling-Henricks M, Villalta SA, et al. IL-10 triggers changes in macrophage phenotype that promote muscle growth and regeneration. J Immunol 2012; 189:3669–3680.

19. Biswas SK, Mantovani A. Macrophage plasticity and interaction with lymphocyte subsets: cancer as a paradigm. Nat Immunol 2010;11:889–896.

20. Xue L, Suzuki H. Electrical responses of gastric smooth muscles in streptozotocin-induced diabetic rats. Am J Physiol 1997;272:G77–G83.

21. Koch KL, Stern RM, Stewart WR, et al. Gastric emptying and gastric myoelectrical activity in patients with diabetic gastroparesis: effect of long-term domperidone treatment. Am J Gastroenterol 1989;84:1069–1075.

22. Chen J, McCallum RW. Gastric slow wave abnormalities in patients with gastroparesis. Am J Gastroenterol 1992; 87:477–482.

23. Chen JD, Lin Z, Pan J, et al. Abnormal gastric myoelectrical activity and delayed gastric emptying in patients with symptoms suggestive of gastroparesis. Dig Dis Sci 1996;41:1538–1545.

24. Cipriani G, Gibbons SJ, Verhulst PJ, et al. Diabetic mice lacking macrophages are protected against the development of delayed gastric emptying. Cell Mol Gastroenterol Hepatol 2016;2:40–47.

25. Miller SM, Reed D, Sarr MG, et al. Haem oxygenase in enteric nervous system of human stomach and jejunum and co-localization with nitric oxide synthase. Neurogastroenterol Motil 2001;13:121–131.

26. Miller SM, Farrugia G, Schmalz PF, et al. Heme oxygenase 2 is present in interstitial cell networks of the mouse small intestine. Gastroenterology 1998;114:239–244.

27. el-Sharkawy TY, Morgan KG, Szurszewski JH. Intracellular electrical activity of canine and human gastric smooth muscle. J Physiol 1978;279:291–307.

28. Farrugia G, Lei S, Lin X, et al. A major role for carbon monoxide as an endogenous hyperpolarizing factor in the gastrointestinal tract. Proc Natl Acad Sci U S A 2003; 100:8567–8570.

29. Huhn RD, Radwanski E, Gallo J, et al. Pharmacodynamics of subcutaneous recombinant human interleukin-10 in healthy volunteers. Clin Pharmacol Ther 1997; 62:171–180.

30. Moore KW, de Waal Malefyt R, Coffman RL, et al. Interleukin-10 and the interleukin-10 receptor. Annu Rev Immunol 2001;19:683–765.

31. Asadullah K, Sterry W, Volk HD. Interleukin-10 therapy–review of a new approach. Pharmacol Rev 2003; 55:241–269.

32. Tilg H, van Montfrans C, van den Ende A, et al. Treatment of Crohn's disease with recombinant human interleukin 10 induces the proinflammatory cytokine interferon gamma. Gut 2002;50:191–195.

33. Buruiana FE, Sola I, Alonso-Coello P. Recombinant human interleukin 10 for induction of remission in Crohn's disease. Cochrane Database Syst Rev 2010;11:CD005109.

34. Robert S, Gysemans C, Takiishi T, et al. Oral delivery of glutamic acid decarboxylase (GAD)-65 and IL10 by Lactococcus lactis reverses diabetes in recent-onset NOD mice. Diabetes 2014;63:2876–2887.

35. Egbuji JU, O'grady G, du P, et al. Origin, propagation and regional characteristics of porcine gastric slow wave activity determined by high-resolution mapping. Neurogastroenterol Motil 2010;22:e292–e300.

36. Lammers WJ, Ver Donck L, Stephen B, et al. Origin and propagation of the slow wave in the canine stomach: the outlines of a gastric conduction system. Am J Physiol Gastrointest Liver Physiol 2009;296:G1200–G1210.

37. O'Grady G, Du P, Cheng LK, et al. Origin and propagation of human gastric slow-wave activity defined by high-resolution mapping. Am J Physiol Gastrointest Liver Physiol 2010;299:G585–G592.

38. Ordog T, Baldo M, Danko R, et al. Plasticity of electrical pacemaking by interstitial cells of Cajal and gastric dysrhythmias in W/W mutant mice. Gastroenterology 2002;123:2028–2040.

39. Kashyap PC, Choi KM, Dutta N, et al. Carbon monoxide reverses diabetic gastroparesis in NOD mice. Am J Physiol Gastrointest Liver Physiol 2010;298:G1013–G1019.

40. Laskin DL, Sunil VR, Gardner CR, et al. Macrophages and tissue injury: agents of defense or destruction? Annu Rev Pharmacol Toxicol 2011;51:267–288.

41. Chen S, Kapturczak MH, Wasserfall C, et al. Interleukin 10 attenuates neointimal proliferation and inflammation in aortic allografts by a heme oxygenase-dependent pathway. Proc Natl Acad Sci U S A 2005;102:7251–7256.

42. Mantovani A, Sica A, Sozzani S, et al. The chemokine system in diverse forms of macrophage activation and polarization. Trends Immunol 2004;25:677–686.

43. Jung M, Sabat R, Kratzschmar J, et al. Expression profiling of IL-10-regulated genes in human monocytes and peripheral blood mononuclear cells from psoriatic patients during IL-10 therapy. Eur J Immunol 2004; 34:481–493.

Correspondence
Address correspondence to: Gianrico Farrugia, MD, Enteric NeuroScience Program, Mayo Clinic, 200 First Street SW, Rochester, Minnesota 55905. e-mail: Farrugia.gianrico@mayo.edu; fax: (507) 284–0266.

Conflicts of interest
This author discloses the following: Jon J. Camp and the Mayo Clinic have a financial conflict of interest with the technology (medical image analysis software) used in this research, and Jon J. Camp and the Mayo Clinic may stand to gain financially from the successful outcome of the research. This technology is not the subject of the research; instead, it is a software tool in the research. The remaining authors disclose no conflicts.